Chemosphere 258 (2020) 127335

Contents lists available at ScienceDirect

Chemosphere

journal homepage: www.elsevier.com/locate/chemosphere

The climate impact on atmospheric stagnation and capability of stagnation indices in elucidating the haze events over North China Plain and Northeast China

Yang Gao [a, b, *], Lei Zhang [a], Ge Zhang [a], Feifan Yan [a], Shaoqing Zhang [c, d, e], Lifang Sheng [e], Jianping Li [c], Minghuai Wang [f], Shiliang Wu [g], Joshua S. Fu [h], Xiaohong Yao [a, b], Huiwang Gao [a, b]

[a] Frontiers Science Center for Deep Ocean Multispheres and Earth System, Key Laboratory of Marine Environment and Ecology, Ministry of Education, Ocean University of China, Qingdao, 266100, China
[b] Laboratory for Marine Ecology and Environmental Science, Qingdao National Laboratory for Marine Science and Technology, Qingdao, 266237, China
[c] Key Laboratory of Physical Oceanography, Ministry of Education, Institute for Advanced Ocean Study, Frontiers Science Center for Deep Ocean Multispheres and Earth System (DOMES), Ocean University of China, Qingdao National Laboratory for Marine Science and Technology, Qingdao, 266100, China
[d] International Laboratory for High-Resolution Earth System Prediction (iHESP), Qingdao, 266237, China
[e] College of Oceanic and Atmospheric Sciences, Ocean University of China, Qingdao, 266100, China
[f] School of Atmospheric Sciences, Nanjing University, Nanjing, 210023, China
[g] Atmospheric Sciences Program, Michigan Technological University, Houghton, MI, 49931, USA
[h] Department of Civil and Environmental Engineering, University of Tennessee, Knoxville, TN, USA

HIGHLIGHTS

- Large variability exists in seasonal mean $PM_{2.5}$ and haze duration and frequency.
- The feasibility of the atmospheric stagnation index (ASI) varies by location.
- In future, the climate models predict a decrease of stagnation in Northeast China.

ARTICLE INFO

Article history:
Received 27 February 2020
Received in revised form
30 May 2020
Accepted 3 June 2020
Available online 10 June 2020

Handling Editor: Xinlei Ge

Keywords:
NCP
NEC
Haze
ASI
RCP 8.5

ABSTRACT

In this study, the spatial pattern and temporal evolution of $PM_{2.5}$ over North China Plain (NCP) and Northeast China (NEC) during 2014–2018 was investigated. The annual mean $PM_{2.5}$ shows clear decreasing trends over time, but the seasonal mean $PM_{2.5}$ as well as the seasonal total duration and frequency of haze days shows large inter-annual fluctuation. Based on the atmospheric stagnation index (ASI), this study examined the correlation between ASI and haze events over NCP and NEC. Detailed analysis indicates that location dependency exists of ASI in the capability of capturing the haze events, and the ability is limited in NCP. Therefore, we first propose two alternative methods in defining the ASI to either account for the lag effect or enlarge the threshold value of wind speed at 500 hPa. The new methods can improve the ability of ASI to explain the haze events over NEC, though marginal improvement was achieved in NCP. Furthermore, this study constructed the equation based on the boundary layer height and wind speed at 10-meter, apparently improving the ability in haze capture rate (HCR), a ratio of haze days during the stagnation to the total haze days. Based on a multi-model ensemble analyses under Representative Concentration Pathway (RCP) 8.5, we found that by the end of this century, climate change may lead to increases in both the duration and frequency of wintertime stagnation events over NCP. In contrast, the models predict a decrease in stagnant events and the total duration of stagnation in winter over NEC.

* Corresponding author. Frontiers Science Center for Deep Ocean Multispheres and Earth System, Key Laboratory of Marine Environment and Ecology, Ministry of Education, Ocean University of China, Qingdao, 266100. China.
E-mail address: yanggao@ouc.edu.cn (Y. Gao).

https://doi.org/10.1016/j.chemosphere.2020.127335
0045-6535/

1. Introduction

With the rapid development of urbanization and industrialization, frequent haze events occurring in China, in particular of the densely populated eastern China, have aroused widespread concern (Huang et al., 2014; Ding et al., 2016; Zhang et al., 2019; Gao et al., 2020). During haze events, the accumulation of particulate matter less than or equal to 2.5 μm in diameter ($PM_{2.5}$) poses serious health, economic and environmental problems. For example, the Global Burden of Disease study by Cohen et al. (2017) found that about 4.2 million people died from long-term exposure to $PM_{2.5}$ globally in 2015, with about a quarter of them from China. Furthermore, in regard to episodic events such as the severe pollution in January 2013 (Ji et al., 2014; Zheng et al., 2015), Mu and Zhang (2013) assessed the direct economic losses of transportation and medical care in China at about 23 billion RMB.

Considering anthropogenic emissions as the important factors affecting the haze formation (Chan and Yao, 2008; Zhou et al., 2010), the Chinese government has recently taken a series of actions to control emissions (Wang and Hao, 2012; Zhao et al., 2013; Tan et al., 2017), resulting in a decline in primary PM and SO_2 since 2006 and a significant drop in NO_x emissions since 2011 (Liu et al., 2016; Li et al., 2017; Wang et al., 2017; Zeng et al., 2019). Despite these reductions in anthropogenic emissions, frequent haze events have occurred in recently years which have been linked to certain meteorological conditions, in particular atmospheric stagnation events (Horton et al., 2012; Hou and Wu, 2016; Cai et al., 2017; Liao et al., 2018).

The atmospheric stagnation event is in general characterized by weak advection and diffusion in horizontal and vertical directions, which is unfavorable for the dispersion of air pollutants (Wang and Angell, 1999; Huang et al., 2018). The Air Stagnation Index (ASI), proposed by Wang and Angell (1999) to delineate the feature of stagnant weather, has been widely used by a number of studies (Leung and Gustafson Jr., 2005; Horton et al., 2012; Horton et al., 2014). Based on the ASI, an atmospheric stagnation day is defined when the daily mean near surface (10 m) wind speed is less than 3.2 m/s, daily total precipitation less than 1 mm and upper-air (500 hPa) wind speed less than 13 m/s. However, when evaluating the relationship between atmospheric stagnation and haze events over China, several recent studies have indicated that the ASI approach may not work well (Huang et al., 2017, 2018; Wang et al., 2018). For instance, Huang et al. (2017) suggested that the deficiency of ASI lies in the threshold of wind speed at 500 hPa attributable to the topographic heterogeneity, and they adjusted the pressure level for the threshold from 500 hPa to 400 hPa and 300 hPa for regions with elevation of 1000–3000 m and 3000–4000 m, respectively. However, this adjustment is not applied in the broad plain areas of eastern China with frequent haze events, and it is thus essential to investigate how ASI may affect or explain the haze events over this region.

Climate change can directly affect weather conditions and hence air quality such as ozone and $PM_{2.5}$ levels (Jacob and Winner, 2009; Gao et al., 2012, 2013; Kim et al., 2014; Fiore et al., 2015; Sun et al., 2015; Zhang et al., 2018; Ma et al., 2019). Future changes of stagnant weather conditions are tightly linked to the frequency of haze occurrence. For example, Cai et al. (2017) pointed out that the days with weather conditions conducive to sever haze episodes in Beijing may increase by 50% by the end of this century (2050–2099) compared to the historical period (1950–1999). Han et al. (2017) estimated that weak ventilation days, which are favorable for haze accumulation, would increase over NEC and BTH at a rate of 2.60%/decade and 2.30%/decade, respectively, which were much larger than in the other two regions (0.88%/decade for YRD and −0.01%/decade for PRD). Therefore, it is of vital interest to investigate how future climate may modulate the meteorological conditions such as the ASI and subsequently affect haze pollution over NCP and NEC.

In what follows, we first analyze the spatial and temporal changes of $PM_{2.5}$ as well as the duration and frequency of haze events in China during 2014–2018. The capability of ASI in explaining the haze events is then discussed. Lastly, the impact of climate change on the ASI days over NCP and NEC is examined based on Coupled Model Intercomparison Project Phase 5 (CMIP5) multi-model ensemble.

2. Data description and method

In this study, we analyze the observational data for hourly $PM_{2.5}$ concentrations during 2014–2018 which are available at http://www.pm25.in. The meteorological data including daily wind speed at 10 m and 500 hPa, daily precipitation and boundary layer height is from ECMWF Interim Reanalysis Data (ERA-Interim (Dee et al., 2011)), with spatial resolution of 1.125° × 1.125°. The stational $PM_{2.5}$ data is interpolated into the same spatial resolution as ERA-Interim to facilitate the analysis.

When displaying the characteristics of $PM_{2.5}$ in the first place, the traditional methods often apply the seasonal or annual mean $PM_{2.5}$ (Fan et al., 2019; Luo et al., 2019), which however, fails to delineate a full picture of the pollution extent. Therefore, we adopted two sophisticated metrics including frequency and duration, commonly used in the examination of extreme weather events (Gao et al., 2012, 2013; Zhang et al., 2018), and these metrics may foster a better understanding of haze events in comparison to a single mean value. In selection of regions, four major economic areas are often used to examine the haze pollution, including of Beijing–Tianjin–Hebei (BTH) or North China Plain (NCP), Yangtze River Delta (YRD), Pearl River Delta (PRD) and Northeast China (NEC). Among these four regions, the northern areas including BTH/NCP and NEC normally face more severe haze pollution in comparison to the other two (YRD and PRD). The larger severity of $PM_{2.5}$ pollution in NCP and NEC can be clearly seen from a few previous studies, i.e., the annual mean $PM_{2.5}$ during 2000–2016 depicted in Fig. 5 and 6 of Luo et al. (2019), a synthesis of $PM_{2.5}$ concentration compiled from a variety of studies shown in Fig. 1 of the review paper by Gautam et al. (2019) as well as an abnormally high pollution period in December 2015 shown in Fig. 1 by Zhang et al. (2019). Thus, this study aims to elucidate the characteristics of annual and seasonal $PM_{2.5}$ as well as the duration and frequency of haze events over NCP and NEC.

The CMIP5 (https://esgf-node.llnl.gov/search/cmip5/) multi-model data is used in this study to investigate the changes of haze related atmospheric stagnation events in China. A total of 20 CMIP5 models (listed in Table 1) are assessed, the daily wind speed of 10 m and 500 hPa and daily precipitation of both historical (1975–2004) and future (2071–2100) period under the scenarios of RCP 8.5 is used in this study. All CMIP5 data are interpolated bilinearly into 1.25° (latitude) × 1.875° (longitude) spatial resolution, the same as our previous studies (Gao et al., 2015, 2016).

3. Results and discussions

3.1. The frequency and duration of haze events in China during 2014–2018

The spatial distribution of seasonal mean $PM_{2.5}$ concentrations in China, as shown in Fig. S1 in the supporting information, indicates high $PM_{2.5}$ levels in winter and the most severe pollution are found over the eastern China, i.e., over the NCP and NEC regions, with the seasonal mean $PM_{2.5}$ concentrations up to 160 μg m^{-3} or

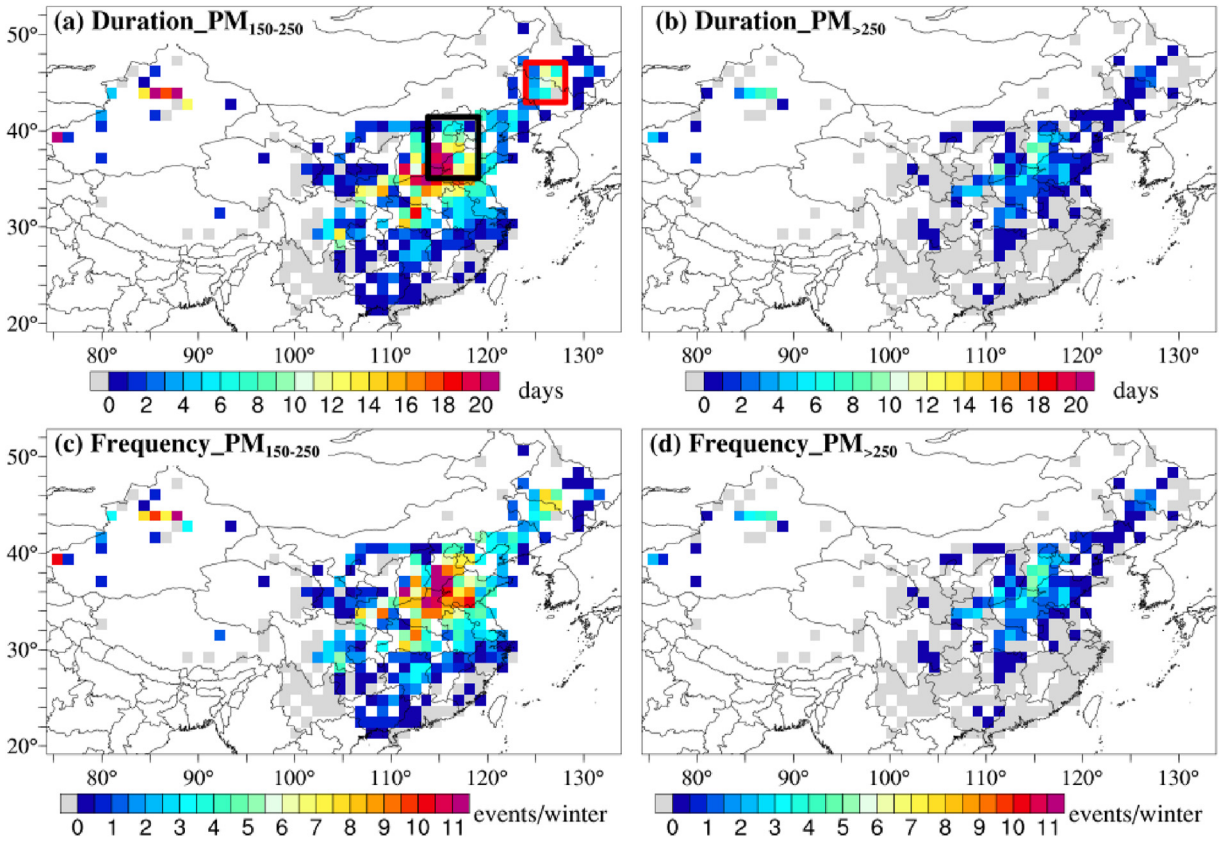

Fig. 1. The seasonal duration (top row) and frequency (bottom row) of the haze events under category V (daily $PM_{2.5}$ of 150–250 μg m^{-3}; left) and VI (daily $PM_{2.5}$>250 μg m^{-3}; right) in winter during 2014–2018. The white areas indicate locations with no observational data and gray areas indicate the value is 0. The black and red boxes denote the regions of NCP and NEC, respectively. (For interpretation of the references to colour in this figure legend, the reader is referred to the Web version of this article.)

Table 1
A list of the CMIP5 models analyzed in this study.

Model	Institution	Resolution (Lon × Lat)
1. ACCESS1.0	Commonwealth Scientific and Industrial Research Organization (CSIRO), Australia and Bureau of Meteorology (BOM), Australia	1.875 × 1.25
2. ACCESS1.3		1.875 × 1.25
3. CanESM2	Canadian Centre for Climate Modeling and Analysis, Canada	2.81 × 2.79
4. CMCC-CM	Euro-Mediterraneo sui Cambiamenti Climatici, Italy	0.75 × 0.75
5. CMCC-CMS		1.875 × 1.86
6. CNRM_CM5	Centre National de Recherches Meteorologiques, Meteo-France, France	1.41 × 1.40
7. CSIRO_Mk3.6.0	Commonwealth Scientific and Industrial Research Organization (CSIRO), Australia	1.875 × 1.86
8. GFDL-ESM2M	NOAA Geophysical Fluid Dynamics Laboratory, USA	2.5 × 2.0
9. GFDL-ESM2G		2.5 × 2.0
10. HadGEM2_CC	Met Office Hadley Centre, UK	1.875 × 1.25
11. INM-CM4	Institute for Numerical Mathematics, Russia	2.0 × 1.5
12. IPSL-CM5A-LR	Institut Pierre-Simon Laplace, France	3.75 × 1.875
13. IPSL-CM5A-MR		2.5 × 1.25
14. IPSL-CM5B-LR		3.75 × 1.875
15. MIROC-ESM	Atmosphere and Ocean Research Institute (The University of Tokyo), National Institute for Environmental Studies and Japan Agency for Marine-Earth Science and Technology	2.81 × 1.77
16. MIROC-ESM-CHEM		2.81 × 1.77
17. MIROC5		1.41 × 1.39
18. MPI-ESM-LR	Max Planck Institute for Meteorology, Germany	1.875 × 1.85
19. MPI-ESM-MR		1.875 × 1.85
20. MRI-CGCM3	Meteorological Research Institute, Japan	1.125 × 1.125

higher (Fig. S1d). These results are consistent in general with the previous studies (An et al., 2019; Fan et al., 2019). Li et al. (2019) investigated the characteristics of $PM_{2.5}$ over two urban agglomerations in Northeast China, including Central Liaoning Urban Agglomeration (CLUA) and Harbin-Changchun Urban Agglomeration (HCUA), and found the highest mean $PM_{2.5}$ concentration during 2015–2017 of 58.3 ± 74.1 μg m^{-3} occurring at Harbin, a large city in HCUA. Considering the larger area and population in HCUA compared to CLUA, the NEC region in this study mainly refers to HCUA area rather than the entire northeast of China. In other seasons (Figs. S1a–c), the spatial heterogeneity care also clear with significantly higher $PM_{2.5}$ in eastern China except in spring and summer when the dust aerosol may lead to much higher $PM_{2.5}$ in northwestern China, i.e., southern Xinjiang (Fan et al., 2019; Yuan et al., 2019).

With the air quality index (AQI) (HJ 633–2012; (MEEPRC, 2012)), the $PM_{2.5}$ air quality can be classified into six categories based on the daily $PM_{2.5}$ average concentrations at a given location/region: I) 0–35 μg m^{-3}, II) 35–75 μg m^{-3}, III) 75–115 μg m^{-3}, IV) 115–150 μg m^{-3}, V) 150–250 μg m^{-3} and VI) greater than 250 μg m^{-3}. In this study, a haze event of category X for a specific model is defined as if the $PM_{2.5}$ air quality over that grid falls in category X or higher for a consecutive period of time. The frequency and duration of category X haze events are calculated as the number of haze events and total number of haze days respectively falling into that categories.

The spatial variations of frequency and duration category V and VI for haze events in winter are shown in Fig. 1, and the results for other seasons including spring, summer and fall shown in Figs. S2–4. We can see that winter is the season with most frequent haze events (Fig. 1 vs. Figs. S2–4), similar to the results from examining the seasonal mean $PM_{2.5}$ concentrations (Fig. S1). Most parts of eastern China have been affected by severe haze in winter, in particular the NCP (black box in Fig. 1a) and the NEC (red box in Fig. 1a) regions. The frequency and duration of haze events under category V and VI over NCP and NEC during all seasons 2014–2018 are listed in Table 2. Based on Table 2 and Fig. 1, Fig. S2–S4, the annual total duration and frequency for haze events in category V is 22.3 days and 14.3 events over NCP, 10.6 days and 7.6 events over NEC, respectively, about 2.9–4.8 times of that in category VI. However, the average duration of each event under these two categories is similar, lasting about 1.4 days. Among the total annual haze days, the occurrence in winter over NCP accounts for more than half, i.e., 59% (13.2 days) for category V and 76% (3.7 days) for category VI. In contrast, over NEC, albeit of the dominant haze occurrence in winter for category V (61%), the total duration in fall (70%) actually surpassed winter (27%) under category VI.

In addition to the spatial distribution of the five-year haze events, the interannual variations of haze events over NCP and NEC from 2014 to 2018 is further explored (Fig. 2). There are a couple of distinct and interesting features. First, from the perspective of annual mean $PM_{2.5}$, both NCP and NEC display monotonic decreasing trends, on average values of −8.0 μg m^{-3} and -5.4 μg m^{-3} per year in NCP and NEC during 2014–2018, consistent with Li et al. (2020) of 10 μg m^{-3} decrease per year over North China during 2013–2017. A large concentration drop can be found over NCP in 2017, with a decrease of 21.7 μg m^{-3} compared to the mean $PM_{2.5}$ in 2014–2016, partly due to the large emission reduction which is visible in Fig. 10a of Fan et al. (2019). From the perspective of seasonal scale, $PM_{2.5}$ mean concentration over NCP in spring, summer and fall shows in general consistent decreasing trend with annual variation, whereas in winter, it increases from 2014 to 2016 with maximal value of 116.6 μg m^{-3} in 2016, followed by a substantial drop in 2017, and increase again in 2018. The abnormal seasonal $PM_{2.5}$ can be viewed more clearly by examining the values in each month (Fig. S5), showing that the high seasonal mean $PM_{2.5}$ in 2015 and 2016 is closely linked to the dramatic concentration enhancement in December of the respective year. The high $PM_{2.5}$ in December 2015 was attributed to the weak dispersion conditions possibly induced by the strong El Niño during that time (Zhang et al., 2019). In contrast, the haze conducive conditions in December 2016 such as low planetary boundary layer and near surface wind speed was likely modulated by the weakened East Asia jet stream in the upper troposphere and positive phase of the East Atlantic–West Russia pattern in the mid-troposphere (Yin and Wang, 2017). Over NEC, a basic decreasing trend from 2014 to 2018 is observable in all seasons, except that in the year of 2017, with lowest mean winter $PM_{2.5}$ concentration among the five-year, and higher concentration in fall relative to the adjacent years. The monthly variation of $PM_{2.5}$ (Fig. S6) indicates that the abnormally high $PM_{2.5}$ in fall 2017 is mainly contributed by the high value in October (Fig. S6c; comparable to the results shown in Fig. 3a of Li et al. (2019)), whereas the apparently low $PM_{2.5}$ in winter 2017 is due to the equivalently low values in all three months over this season (Fig. S6d).

Besides to the annual or seasonal mean $PM_{2.5}$, it is important to quantify the occurrence of severe pollution cases. Thus, the regional mean duration, frequency and length of each event with $PM_{2.5}$ greater than 150 μg m^{-3} over NCP and NEC is shown in Fig. 2b–d, with seasonal total duration and frequency of $PM_{2.5}$ for categories I to VI listed in Tables S1–4. The annual total duration and frequency in both NCP and NEC tends to decrease from 2014 to 2018, consistent with the trend of the annual mean $PM_{2.5}$. The annual mean event length shows slightly increasing trend over NCP, opposite to that in NEC. However, larger variability is discernable when seasonal changes are evaluated. For instance, although a general decreasing trend is observable in the haze duration and frequency over NCP, fluctuation exists in the seasonal variation rather than a monotonic decrease. In regard of NEC, the magnitude of fluctuation is even larger. The haze duration over NEC in fall is 6.4 days in 2017, whereas it decreases to 2.0 days in 2016 and disappears in 2018; In contrast, the winter of 2017 yields the duration of 1.4 days, much smaller than the other four years ranging from 5.6 days to 7.9 days.

Table 2
The five-year (2014–2018) mean duration and frequency of haze events for category V (150–250 μg m^{-3}) and VI (>250 μg m^{-3}) averaged over NCP and NEC during 2014–2018.

Season	Region	Duration (days)		Frequency (events)	
		Category V	Category VI	Category V	Category VI
Spring	NCP	3.2	0.3	2.3	0.2
	NEC	0.7	0.1	0.5	0.1
Summer	NCP	0.6	0	0.4	0
	NEC	0.3	0	0.1	0
Fall	NCP	5.3	0.9	3.5	0.6
	NEC	3.2	2.6	2.5	1.7
Winter	NCP	13.2	3.7	8.2	2.2
	NEC	6.5	1.0	4.5	0.8
Annual	NCP	22.3	4.9	14.3	3.0
	NEC	10.6	3.7	7.6	2.6

3.2. The capability of ASI in explaining the haze events over NCP and NEC

To investigate the influence of the atmospheric stagnation on $PM_{2.5}$ concentration over NCP and NEC, we firstly define, for any particular grid, the days less than the thresholds of ASI referred to as stagnation, and all the other days referred to as non-stagnation.

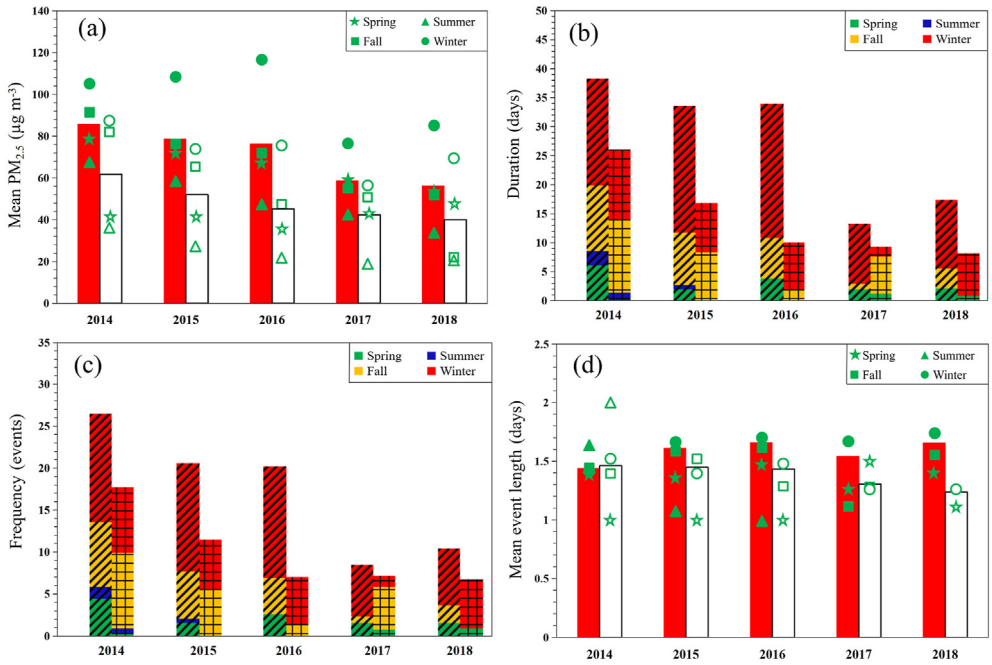

Fig. 2. The annual (histogram) and seasonal (green markers) mean $PM_{2.5}$ concentration (a), as well as the seasonal total duration (b), frequency (c), annual (histogram) and seasonal mean (green markers) length of each event (d) for haze events ($PM_{2.5}$ > 150 μg m^{-3}; including both category V and VI), over NCP (left of each sub-panel) and NEC (right of each sub-panel) during 2014–2018. (For interpretation of the references to colour in this figure legend, the reader is referred to the Web version of this article.)

The thresholds of ASI are that the daily mean 10-m wind speed, daily mean 500 hPa wind speed and daily total precipitation at 3.2 m/s, 13 m/s and 1 mm, respectively, the same as the previous study (Horton et al., 2014). The mean $PM_{2.5}$ during stagnation and non-stagnation in each season of 2014–2018 is shown in Table 3. The mean $PM_{2.5}$ concentration during the stagnation is in general significantly higher than that over the non-stagnation with statistical difference ($P < 0.05$), except that no significant differences exist in summer NEC and significantly lower during stagnation is observed than non-stagnation days in fall over NEC. The $PM_{2.5}$ differences can also be identified from the probability distribution function (PDF) of the composited $PM_{2.5}$ during stagnation and non-stagnation (Fig. S7), and the exception discussed above regarding the summer and fall over NEC is clearly depicted in Fig. S7 that the probability of $PM_{2.5}$ concentration over the summer and fall in NEC shows reversed feature. Meanwhile, stagnation fails to capture a large amount days with high $PM_{2.5}$ concentration, indicating the weakness of ASI in explaining the haze day. To further unveil the consistency between the values of daily total precipitation, daily mean wind speed at 10 m and 500 hPa and the thresholds used to define ASI, Fig. 3 displays their cumulative probability distribution (CDF) during the days with mean $PM_{2.5}$ concentration greater than 150 μg m^{-3} over NCP and NEC.

Based on the CDF, a five-year (2014–2018) average of 94% and 99% of daily precipitation (Fig. 3a and b), and 87% and 65% of 10-m wind speed (Fig. 3c and d) over NCP and NEC falls below the threshold used in ASI, which is 1 mm/day for daily precipitation and 3.2 m/s for daily 10-m wind speed. However, in terms of the wind speed at 500 hPa, the threshold of 13 m/s only accounts for 22% and 35% of haze days (i.e., $PM_{2.5}$> 150 μg m^{-3}) over NCP and NEC, respectively. A similar finding was also illustrated by Huang et al. (2018), who found three quarters of the days during high Air pollution index (i.e., 90th percentile or higher) with wind speed at 500 hPa larger than 13 m/s over Beijing during October–March 2000–2012. We also display the CDF of daily precipitation, wind speed at 10-m and 500 hPa during a longer period from 1989 to 2018 (Fig. S8), which supports this finding as well.

To quantitatively measure to what extent the stagnation days based on the atmospheric stagnation index matches the haze days, haze capture rate (HCR) was used to represent the ratio of haze days during stagnation to total haze days, and the spatial distribution of HCR in winter during 2014–2018 is shown in Fig. 4a. The haze day is defined as a day exceeding a certain threshold which we first set as 150 μg m^{-3} to cover the category V and VI based on AQI. The HCR is less than 40% in most regions, and only a few scattered spots in central China may reach 90% or so. The average HCR is 38% over NEC and 7% over NCP, respectively. In particular, the HCR in Beijing is 15%, albeit of slightly smaller, generally consistent with previous finding in Cai et al. (2017), showing that the ASI only capture 28% of the severe haze events in the megacity Beijing in the winter from 2009 to 2015. Therefore, The ASI has limited ability in explaining the haze events, and this capability show large spatial heterogeneity at least in view of NCP and NEC. Re-examining the composited method of exact temporal match between ASI and haze day, as well as the CDF of 500 hpa wind speed shown in Fig. 3, we propose two alternative methods aiming to increase the HCR so as to improve the ability of explaining haze events due to stagnation. In regard of

Table 3
Daily mean $PM_{2.5}$ concentration during the atmospheric stagnation and non-stagnation days for NCP and NEC in each season during 2014–2018.

Season	Region	Seasonal mean $PM_{2.5}$ (μg m^{-3})	
		Stagnation	Non-stagnation
Spring	NCP	71.0	65.2
	NEC	45.9	41.3
Summer	NCP	53.8	48.2
	NEC	24.5	24.7
Fall	NCP	73.3	68.6
	NEC	48.6	53.9
Winter	NCP	102.6	98.9
	NEC	108.2	67.6

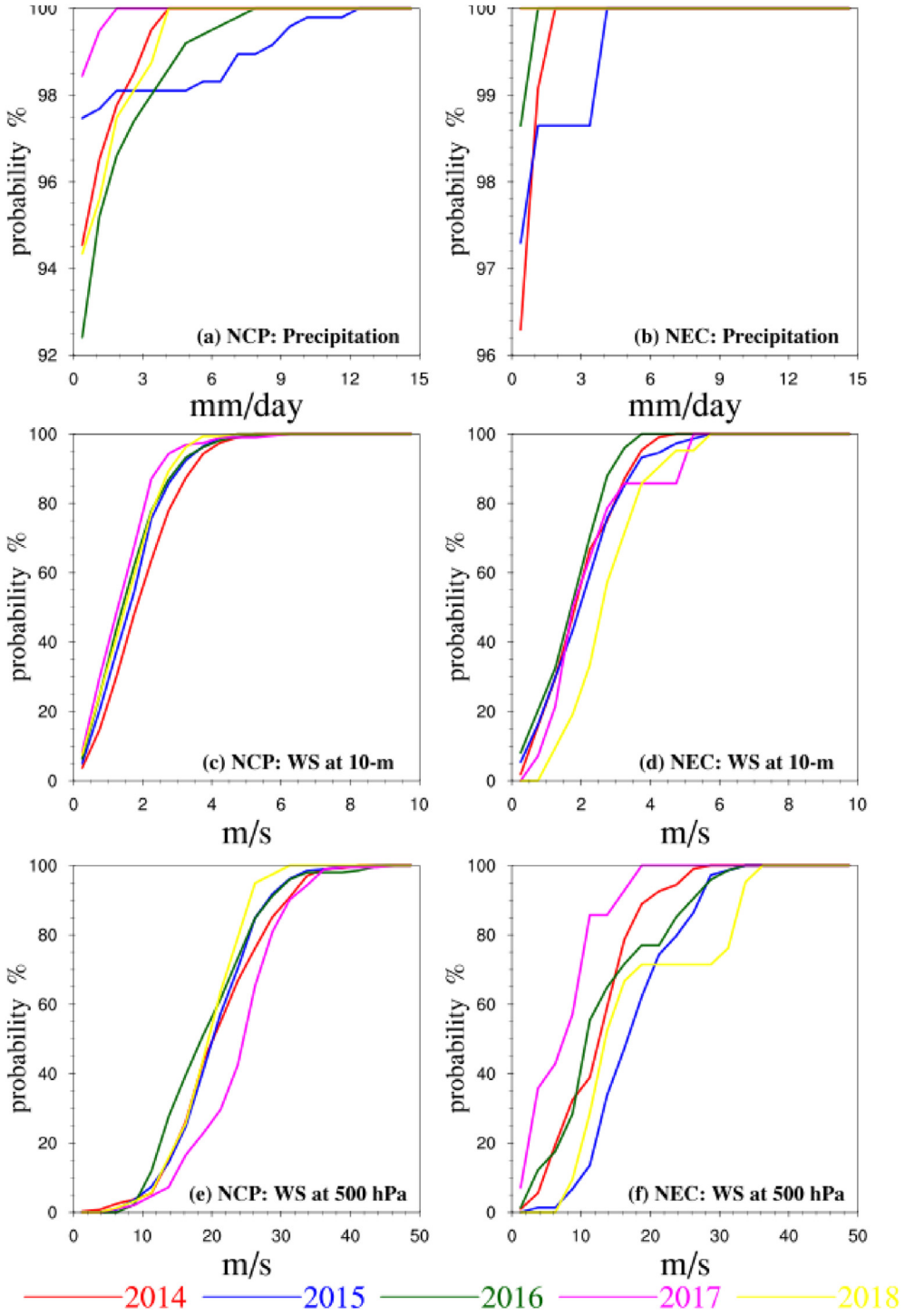

Fig. 3. Cumulative probability distributions of composited daily precipitation, wind speeds at 10-m and 500 hPa respectively, when $PM_{2.5}$ > 150 μg m^{-3} for NCP (left) and NEC (right) during 2014–2018.

the temporal match, it is reasonable to assume that a day lag might exist between stagnation and haze. Based on this assumption, for any specific stagnant day, the haze occurring either on the same day or one day later is considered to be captured by the stagnation. Based on this method (referred to as ASI-lag), the HCR of ASI-lag is shown in Fig. 4b. Compared to the original composite method, ASI-lag does show improvement to a certain degree, i.e., HCR increased from 7% to 15% and from 38% to 60% for NCP and NEC, respectively. Therefore, the ASI-lag might be taken into consideration when applicable. Nevertheless, for NCP, the fraction explained is still low, which is attributable to low threshold of 500 hPa wind speed, leading to a possible improvement method by enlarging the threshold (referred to as ASI-500). A simple test is done by increasing the threshold of wind speed at 500 hPa used in ASI from 13 m/s to 20 m/s with an interval of 1 m/s, and the resulting HCR shows monotonic increase from 7% to 36% in NCP and 38%–67% in

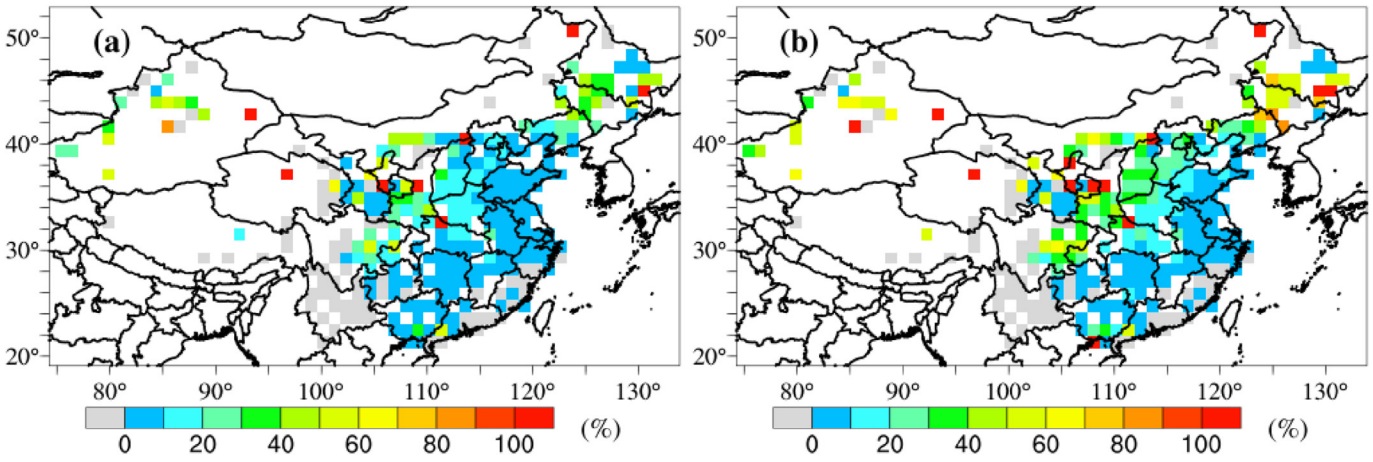

Fig. 4. The haze capture rate, which is the proportion of haze days in the atmospheric stagnation days defined by original ASI (left) and lag considered (right) to total heavy haze days (exceeding 150 μg m^{-3}) in winter during 2014–2018.

NEC based on the five-year (2014–2018) average. However, cautions may be aroused for the method of ASI-500, and a general rule to increment the wind speed at 500 hPa can be linked to the CDF shown in Fig. 3, i.e., the median or even larger threshold displayed in Table S5 may be applied to achieve a satisfactory capability of explaining haze events. Please note that ASI-lag and ASI-500 was applied independently during the test, and one may expect a larger improvement if these two methods were combined. Nevertheless, the ASI fits much better in NEC compared to NCP from either perspective. Please also note that the spatial resolution in Fig. 4 was based on 1.125°, and to exclude the influence due to the coarse resolution, the same analysis was conducted using a finer resolution grid of 0.5°, in general yielding comparable results (not shown).

3.3. *Capabilities and limitations of different atmospheric stagnation indices in elucidating the stagnation and haze events*

Considering that the deficiency of ASI in explaining the haze events mainly lies in the wind speed at 500 hPa, an alternative parameter of boundary layer height (BLH) has been proposed by Wang et al. (2018), in which an equation was derived based on BLH and WS10 to fit the daily $PM_{2.5}$ normalized by the respective monthly mean over United States, Europe and China. Note that the daily precipitation was always set to be 1 mm or lower. Multiple curves can be fitted and based on the interest, Wang et al. (2018) displayed the 100% fitting curve. Based on this fitting equation and the associated stagnation days, Liao et al. (2018) found that during the winter of 2013 and 2015, the $PM_{2.5}$ in southwestern China during the stagnation is on average of about 1.4 times as high as that during non-stagnation, implicative of the effect of stagnation on the enhancement of $PM_{2.5}$. However, the uncertainty apparently exists in the applications to different locations since this fitting curve is the combination of data from several countries. Moreover, while it is important to quantify the ability of stagnation index based on HCR, it is also useful to evaluate the ratio of haze days during the stagnation to the total number of stagnation days, which can be named as the haze stagnation ratio (HSR). It is easy to imagine that if one artificially defines every day as a stagnation day during a certain period, the HCR would always be 100%, but the HSR would be very low. Thus, high HCR and HSR is desirable in search of a good stagnation index in determining the haze events, and to our knowledge, no study has fully discussed in detail the effectiveness of the atmospheric stagnation indices in this manner. To this end, we construct a comprehensive evaluation of the capability and limitation of the indices in the interpretation of haze events.

Since Wang et al. (2018) derived the fitting equation based on BLH and WS10 using the data from different countries, we first make a comparison by applying exactly the same fitting method as Wang et al. (2018) but using data in China, and the fitting line is shown in Fig. 5a. To test the robustness of the fitting, the HCR and HSR is applied for three haze categories, corresponding to the $PM_{2.5}$ concentration of 75 μg m^{-3} (Fig. 6), 115 μg m^{-3} (Fig. S9) and 150 μg m^{-3} (Fig. S10), respectively, with HCR and HSR directly based on Wang et al. (2018) shown in Fig. 6ab. In terms of the three haze categories, the HCR (Fig. 6a vs. Fig. S9a and Fig. S10a) tends to increase when $PM_{2.5}$ concentration is higher, but HSR (Fig. 6b vs. Fig. S9b and Fig. S10b) may decrease. For instance, based on Wang et al. (2018), the average HCR over NCP is 71%, 75% and 79% for $PM_{2.5}$ concentration at 75 μg m^{-3}, 115 μg m^{-3} and 150 μg m^{-3} (Fig. 6a, Fig. S9a, Fig. S10a), while the HSR is 60%, 39% and 25% (Fig. 6b, Fig. S9b, Fig. S10b), respectively. In contrast, by revising the fitting based on the data in China, the HCR over NCP increased by 8%–10% (Fig. 6a, Fig. S9a and Fig. S10a vs. Fig. 6c, Fig. S9c and Fig. S10c; Table S6), while maintaining the HSR similar as Wang et al. (2018) albeit of slightly decrease by less than 4%. The similar feature is observable for regions such as NEC, Yangtze River Delta (YRD), Pearl River Delta (PRD) as well as the entire China (Table S6).

In addition to the fitting of daily $PM_{2.5}$ based on the normalization of monthly mean $PM_{2.5}$, a similar fitting was conducted directly using daily mean $PM_{2.5}$ concentration (Fig. 5c). Correspondingly, HCR and HSR was shown in Fig. 6e and f. Moreover, for the sake of climate studies, it might be useful to conduct normalization using the long term seasonal mean instead of monthly mean, with the fitting shown in Fig. 5e and the differences of HCR and HSR relative to the results based on monthly normalization shown in Fig. 6g and h (Figures. S9g,h, s10g,h). While HCR based on seasonal normalization is in general compared to that from monthly normalization, the overall HCR in China based on the direct $PM_{2.5}$ concentration shows decrease of 7%–9% relative to the monthly normalization. Therefore, the long-term seasonal normalization method will be applied in the following discussions. The fitting method of evaluating the dependence of $PM_{2.5}$ on BLH and WS10, we also examined the influence of WS500 and WS10 (Fig. S11). Whereas there is slight decrease of 8%–13% for HCR in NCP and NEC (Figs. S11g–i), the changes in HSR is negligible (Fig. S11j-l). Therefore, in the case of BLH is not available, the WS500 may also be used as a substitute in this fitting relationship.

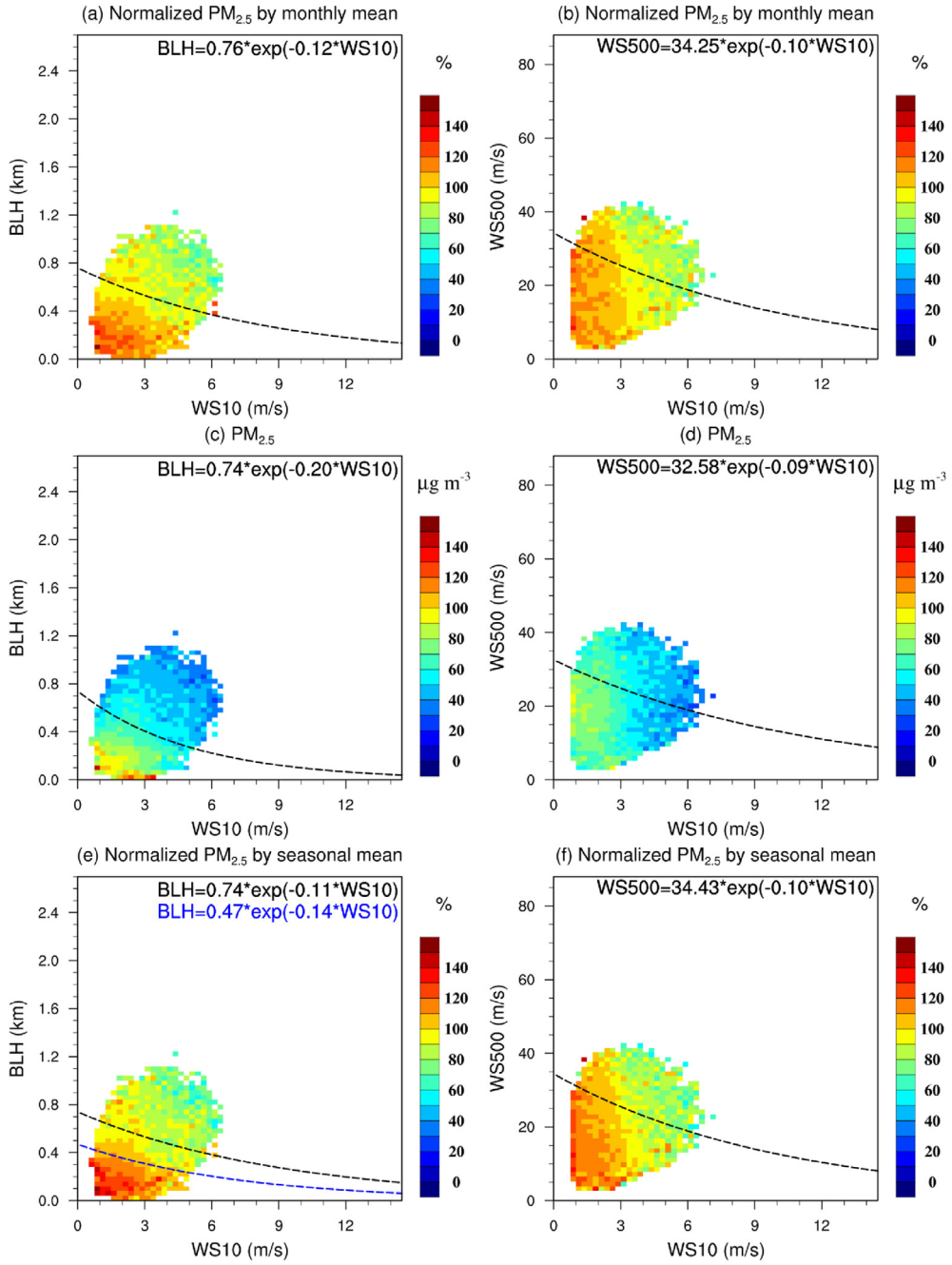

Fig. 5. The distribution of normalized daily $PM_{2.5}$ concentrations by the monthly mean (top row), daily $PM_{2.5}$ concentrations (middle row), and 5-year winter mean (bottom row) based on the 10 m wind speed (WS10) and BLH (left column), WS10 and 500 hPa wind speed (right column) during winter 2014–2018 over China. Only the days with daily precipitation less than 1 mm were selected. Each pixel inside the panel represents the mean daily $PM_{2.5}$ concentration, conducted with at least 20 sample sizes, in each small bin of the WS10 (0.25 m/s), BLH (0.04 km), and WS500 (1.3 m/s).

Besides the fitting line at 100%, it is interesting to test the sensitivity of HCR and HSR to the line selection. Therefore, we fit a blue line in Fig. 5e, with HCR and HSR shown in Fig. S12. The results show a decrease in HCR (Figs. S12g–i), increase in the HSR (Fig. S12j-l), with the magnitude of increase in HSR stronger. i.e., over the entire China, the HCR decreased by 23%–28% (Figs. S12g–i), while the HSR increased by less than 6% (Fig. S12j-l). Therefore, a tradeoff in the selection of the fitting curve might exist and the different signs in the changes in HCR and HSR may indicate the selection of fitting curve may rely on different applications.

In addition to fit by using the data from the entire China, one might think that if we directly fit the line using the observational data in NCP or NEC, the HCR and HSR might be higher. The fitting curve (Fig. S13) based on the data over NCP and NEC and the corresponding HCR and HSR is shown in Figs. S14–15. The basic finding is that HCR decrease by 10–20% whereas the HSR increases by a few percent. The increase in HSR matches our hypothesis, however, the decrease in HCR is unexpected. This phenomenon implies the uncertainty associated with this index and may deserve further investigation in future when applicable.

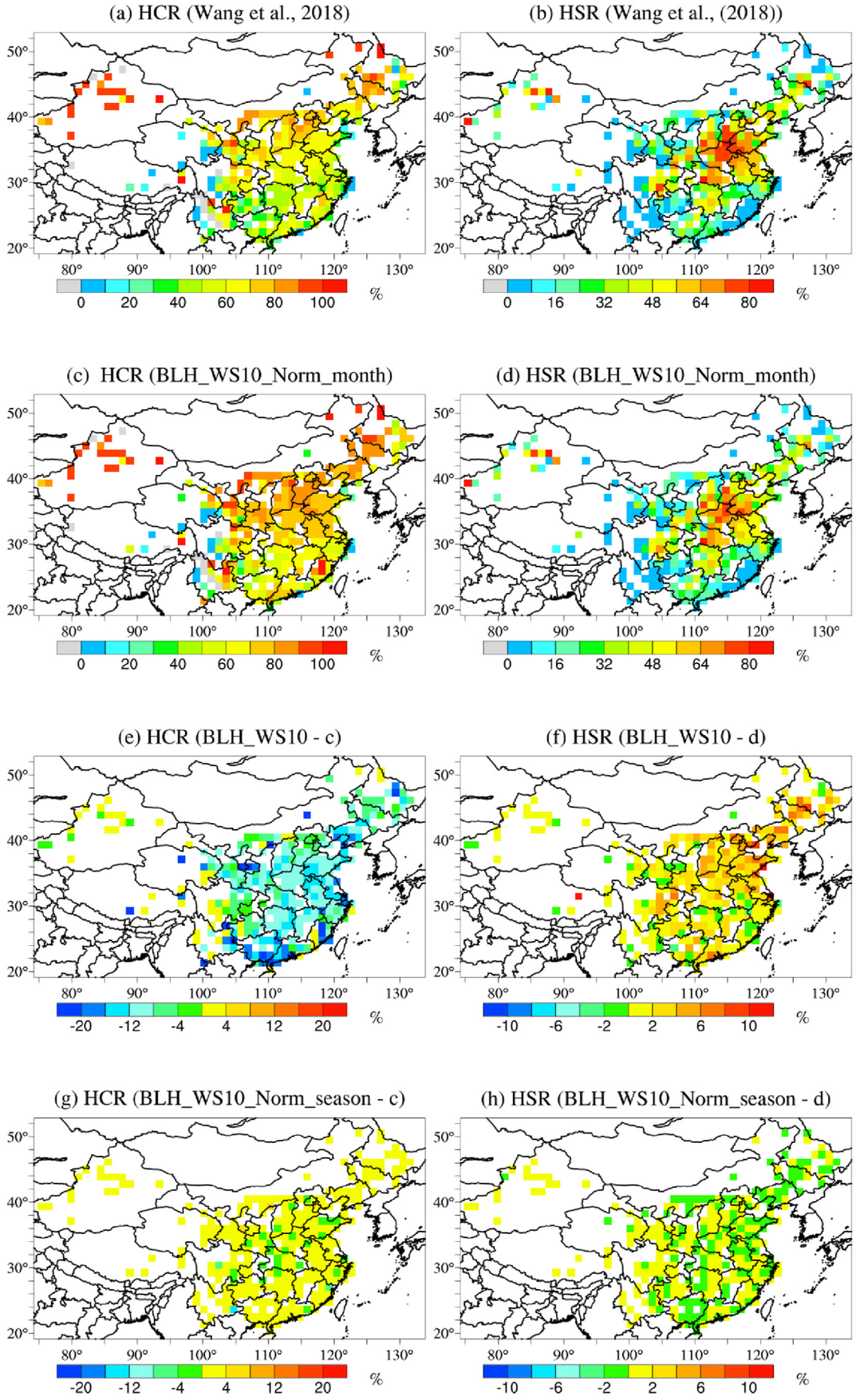

Fig. 6. The HCR (Fig. 6a and c) and HSR (Fig. 6b and d) by Wang et al. (2018) (Fig. 6a–b) and BLH_WS10_Norm_month (Fig. 6c–d) as well as the difference between BLH_WS10 (Fig. 6e–f), BLH_WS10_Norm_season (Fig. 6g–h) and BLH_WS10_Norm_month. The definition of haze days is $PM_{2.5}$>75 μg m^{-3}.

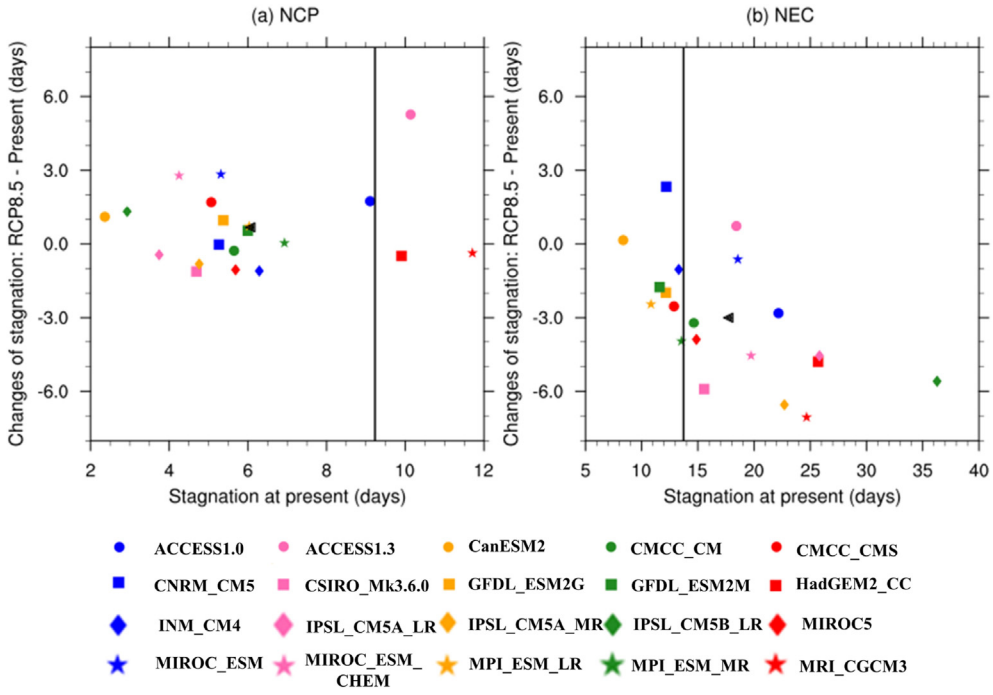

Fig. 7. Future changes of atmospheric stagnation days over NCP (a) and NEC (b) based on 20 CMIP5 model. Abscissa is the average number of days of atmospheric stagnation in winter during the historical period (1975–2004), and ordinate is the difference of atmospheric stagnation days between future (2071–2100) under RCP 8.5 and historical period. The black triangle represents the mean value of 20 CMIP5 models, and other markers indicate values for each model. The black vertical line implies the value from the ERA-Interim (1979–2004).

3.4. Future changes of atmospheric stagnation

It has been inferred from the previous studies (Horton et al., 2014; Zhang et al., 2018) under climate change, the atmospheric stagnation events may be projected to increase in many regions. However, these studies did not examine the changes of stagnation days in winter, which is high likely to be connected with haze pollution over NCP and NEC. Therefore, by taking advantage of the historical (1975–2004) and future (2071–2100, under RCP 8.5 scenario) period results of the CMIP5 multi-model ensemble, the impact of climate change on atmospheric stagnation is investigated. We first examine the future changes of atmospheric stagnation duration based on the standard ASI (Horton et al., 2014). The total number of stagnation days in winter from each of the 20 CMIP5 models as well as the reanalysis data ERA-Interim (1979–2004) is shown in Fig. 7. The starting year of ERA-Interim is 1979 due to the data availability. The duration of stagnation over NCP and NEC is 9.2 days and 13.7 days based on ERA-Interim, whereas the CMIP5 generally performs reasonably well, with multi-model mean duration of 6.1 days and 17.7 days in these two regions, respectively.

By the end of the century, the stagnation days over NCP in winter is projected to increase by 0.7 days, yet with low model agreement, i.e., 11 models of 20 models agree with the mean signal. In contrast, over NEC, the CMIP5 models robustly (17 models show negative sign) show a decrease of stagnation, with mean value of 3.0 days in winter. This finding is further supported by the analysis of stagnation based on the equation in Fig. 5f, yielding comparable future changes for both NCP and NEC in winter. Note that as mentioned earlier, the index leads to increase of historical stagnation a few times compared to the index based on Horton et al. (2014), and such a large number of stagnation days may not necessarily correspond to the haze days. Nevertheless, the consistent signal of changes in stagnation enhances the confidence in interpreting the future changes as well as the haze pollution associated with it. Over NEC, the results in this study is somewhat different from the study of Han et al. (2017), in which the air weak ventilation days increase in winter is projected. The inconsistency is possibly due to the differences in the index selection (stagnation in our study vs weak ventilation days in Han et al. (2017)) or model discrepancies, i.e., 20 CMIP5 models used in this study vs one regional model driven by three global climate models. Nevertheless, the climate impact illustrated in this study is vital to take into consideration in future air quality management.

4. Conclusions

This study first investigated the spatial and temporal characteristics of haze events over two regions in China where there have been frequent haze events, including NCP and NEC. Consistent with previous studies, the annual mean $PM_{2.5}$ over these regions in general depicts a decreasing trend in the past years. However, further analysis focusing on the seasonal variability of haze events and statistical analysis examining the duration and frequency of various categories of haze events revealed some unique features. The seasonal average $PM_{2.5}$ concentrations do not always show the decreasing trend during the 2014–2018 period, as observed with the annual mean $PM_{2.5}$ concentrations. For example, the winter mean $PM_{2.5}$ over NCP were increasing from 2014 to 2016. The total number of haze days in fall 2017 is much higher than either 2016 or 2018, whereas in winter, it is much lower than any of the other years. This implies that when examining the seasonal average $PM_{2.5}$ concentrations, the inter-annual variations in air quality driven by the inter-annual variations in meteorology dominates over the general reduction driven by emission control.

The atmospheric stagnation index was recently pointed out for the shortcoming in explaining the haze events. In this study, we make a further step to compare its capability in capturing haze

events in two regions including NEC and NCP, and found that ASI works much better in NEC than NCP. Two alternative methods through the incorporation of either a day lag effect or enlarging the threshold of wind speed at 500 hPa are proposed, which did substantially improve the ability in explaining the haze events. Moreover, the capability and limitations of atmospheric stagnation indices, by incorporating the BLH, WS500 and WS10, were comprehensive evaluated. Whereas the index with BLH and WS10 generally yields better performance in explaining the haze events, we emphasize that it is necessary to take into account of both HCR and HSR. In future, the CMIP5 multi-model ensemble predicts an increase of stagnation days over NCP and decrease of stagnation days over NEC, with the latter more robust and stronger model agreement. Albeit of the uncertainties exist, these results imply that future climate modulation on the stagnant weather patterns may vary by region, which is important to take into consideration in future air quality related policies.

Declaration of competing interest

The authors declare that they have no conflict of interest.

CRediT authorship contribution statement

Yang Gao: Conceptualization, Methodology, Writing - original draft. **Lei Zhang:** Visualization, Formal analysis, Writing - review & editing. **Ge Zhang:** Visualization. **Feifan Yan:** Validation, Formal analysis, Writing - review & editing. **Shaoqing Zhang:** Writing - review & editing. **Lifang Sheng:** Writing - review & editing. **Jianping Li:** Writing - review & editing. **Minghuai Wang:** Visualization, Writing - review & editing. **Shiliang Wu:** Writing - review & editing. **Joshua S. Fu:** Validation. **Xiaohong Yao:** Validation. **Huiwang Gao:** Writing - review & editing.

Acknowledgement

This research was supported by grants from the National Natural Science Foundation of China (91744208, 41705124). The analysis was performed using the computing resources of Center for High Performance Computing and System Simulation, Pilot National Laboratory for Marine Science and Technology (Qingdao).

Appendix A. Supplementary data

Supplementary data to this article can be found online at https://doi.org/10.1016/j.chemosphere.2020.127335.

References

An, Z., Zhang, R., Tie, X., Li, G., Cao, J., Zhou, W., Shi, Z., Han, Y., Gu, Z., Ji, Y., 2019. Severe haze in northern China: a synergy of anthropogenic emissions and atmospheric processes. Proc. Natl. Acad. Sci. Unit. States Am. 116, 8657–8666. https://doi.org/10.1073/pnas.1900125116.

Cai, W., Li, K., Liao, H., Wang, H., Wu, L., 2017. Weather conditions conducive to Beijing severe haze more frequent under climate change. Nat. Clim. Change 7, 257–262. https://doi.org/10.1038/nclimate3249.

Chan, C.K., Yao, X., 2008. Air pollution in mega cities in China. Atmos. Environ. 42, 1–42. https://doi.org/10.1016/j.atmosenv.2007.09.003.

Cohen, A.J., Brauer, M., Burnett, R., Anderson, H.R., Frostad, J., Estep, K., Balakrishnan, K., Brunekreef, B., Dandona, L., Dandona, R., Feigin, V., Freedman, G., Hubbell, B., Jobling, A., Kan, H., Knibbs, L., Liu, Y., Martin, R., Morawska, L., Pope III, C.A., Shin, H., Straif, K., Shaddick, G., Thomas, M., van Dingenen, R., van Donkelaar, A., Vos, T., Murray, C.J.L., Forouzanfar, M.H., 2017. Estimates and 25-year trends of the global burden of disease attributable to ambient air pollution: an analysis of data from the Global Burden of Diseases Study 2015. Lancet 389, 1907–1918. https://doi.org/10.1016/s0140-6736(17)30505-6.

Dee, D.P., Uppala, S.M., Simmons, A.J., Berrisford, P., Poli, P., Kobayashi, S., Andrae, U., Balmaseda, M.A., Balsamo, G., Bauer, P., Bechtold, P., Beljaars, A.C.M., van de Berg, L., Bidlot, J., Bormann, N., Delsol, C., Dragani, R., Fuentes, M., Geer, A.J., Haimberger, L., Healy, S.B., Hersbach, H., Holm, E.V., Isaksen, L., Kallberg, P., Koehler, M., Matricardi, M., McNally, A.P., Monge-Sanz, B.M., Morcrette, J.J., Park, B.K., Peubey, C., de Rosnay, P., Tavolato, C., Thepaut, J.N., Vitart, F., 2011. The ERA-Interim reanalysis: configuration and performance of the data assimilation system. Q. J. R. Meteorol. Soc. 137, 553–597. https://doi.org/10.1002/qj.828.

Ding, A.J., Huang, X., Nie, W., Sun, J.N., Kerminen, V.M., Petaja, T., Su, H., Cheng, Y.F., Yang, X.Q., Wang, M.H., Chi, X.G., Wang, J.P., Virkkula, A., Guo, W.D., Yuan, J., Wang, S.Y., Zhang, R.J., Wu, Y.F., Song, Y., Zhu, T., Zilitinkevich, S., Kulmala, M., Fu, C.B., 2016. Enhanced haze pollution by black carbon in megacities in China. Geophys. Res. Lett. 43, 2873–2879. https://doi.org/10.1002/2016gl067745.

Fan, H., Zhao, C., Yang, Y., 2019. A comprehensive analysis of the spatio-temporal variation of urban air pollution in China during 2014-2018. Atmos. Environ. 220 https://doi.org/10.1016/j.atmosenv.2019.117066.

Gao, Y., Fu, J., Drake, J., Liu, Y., Lamarque, J.-F., 2012. Projected changes of extreme weather events in the eastern United States based on a high resolution climate modeling system. Environ. Res. Lett. 7, 044025 https://doi.org/10.1088/1748-9326/7/4/044025.

Fiore, A., Naik, V., Leibensperger, E., 2015. Air quality and climate connections. J. Air Waste Manag. Assoc. 65, 645–685. https://doi.org/10.1080/10962247.2015.1040526, 2015.

Gao, Y., Fu, J.S., Drake, J.B., Lamarque, J.F., Liu, Y., 2013. The impact of emission and climate change on ozone in the United States under representative concentration pathways (RCPs). Atmos. Chem. Phys. 13, 9607–9621. https://doi.org/10.5194/acp-13-9607-2013.

Gao, Y., Lu, J., Leung, L., Yang, Q., Hagos, S., Qian, Y., 2015. Dynamical and thermodynamical modulations on future changes of landfalling atmospheric rivers over western North America: projections of Atmospheric River Changes. Geophys. Res. Lett. n https://doi.org/10.1002/2015GL065435. /a-n/a.

Gao, Y., Lu, J., Leung, L., 2016. Uncertainties in projecting future changes in atmospheric rivers and their impacts on heavy precipitation over Europe. J. Clim. 29 https://doi.org/10.1175/JCLI-D-16-0088.1.

Gao, Y., Shan, H., Zhang, S., Sheng, L., Li, J., Zhang, J., Ma, M., Meng, H., Luo, K., Gao, H., Yao, X., 2020. Characteristics and sources of PM2.5 with focus on two severe pollution events in a coastal city of Qingdao, China. Chemosphere 247. https://doi.org/10.1016/j.chemosphere.2020.125861, 125861-125861.

Gautam, S., Patra, A.K., Kumar, P., 2019. Status and chemical characteristics of ambient PM2.5 pollutions in China: a review. Environ. Dev. Sustain. 21, 1649–1674. https://doi.org/10.1007/s10668-018-0123-1.

Han, Z., Zhou, B., Xu, Y., Wu, J., Shi, Y., 2017. Projected changes in haze pollution potential in China: an ensemble of regional climate model simulations. Atmos. Chem. Phys. 17, 10109–10123. https://doi.org/10.5194/acp-17-10109-2017.

Horton, D.E., Harshvardhan, Diffenbaugh, N.S., 2012. Response of air stagnation frequency to anthropogenically enhanced radiative forcing. Environ. Res. Lett. 7 https://doi.org/10.1088/1748-9326/7/4/044034.

Horton, D.E., Skinner, C.B., Singh, D., Diffenbaugh, N.S., 2014. Occurrence and persistence of future atmospheric stagnation events. Nat. Clim. Change 4, 698–703. https://doi.org/10.1038/nclimate2272.

Hou, P., Wu, S., 2016. Long-term changes in extreme air pollution meteorology and the implications for air quality. Sci. Rep. 6 https://doi.org/10.1038/srep23792.

Huang, Q., Cai, X., Song, Y., Zhu, T., 2017. Air stagnation in China (1985-2014): climatological mean features and trends. Atmos. Chem. Phys. 17, 7793–7805. https://doi.org/10.5194/acp-17-7793-2017.

Huang, Q., Cai, X., Wang, J., Song, Y., Zhu, T., 2018. Climatological study of the Boundary-layer air Stagnation Index for China and its relationship with air pollution. Atmos. Chem. Phys. 18, 7573–7593. https://doi.org/10.5194/acp-18-7573-2018.

Huang, R.-J., Zhang, Y., Bozzetti, C., Ho, K.-F., Cao, J.-J., Han, Y., Daellenbach, K.R., Slowik, J.G., Platt, S.M., Canonaco, F., Zotter, P., Wolf, R., Pieber, S.M., Bruns, E.A., Crippa, M., Ciarelli, G., Piazzalunga, A., Schwikowski, M., Abbaszade, G., Schnelle-Kreis, J., Zimmermann, R., An, Z., Szidat, S., Baltensperger, U., El Haddad, I., Prevot, A.S.H., 2014. High secondary aerosol contribution to particulate pollution during haze events in China. Nature 514, 218–222. https://doi.org/10.1038/nature13774.

Jacob, D., Winner, D., 2009. Effect of climate change on air quality. Atmos. Environ. 43 https://doi.org/10.1016/j.atmosenv.2008.09.051.

Ji, D., Li, L., Wang, Y., Zhang, J., Cheng, M., Sun, Y., Liu, Z., Wang, L., Tang, G., Hu, B., Chao, N., Wen, T., Miao, H., 2014. The heaviest particulate air-pollution episodes occurred in northern China in January, 2013: insights gained from observation. Atmos. Environ. 92, 546–556. https://doi.org/10.1016/j.atmosenv.2014.04.048.

Kim, Y.-M., Zhou, Y., Gao, Y., Fu, J., Johnson, B., Huang, C., Liu, Y., 2014. Spatially resolved estimation of ozone-related mortality in the United States under two Representative Concentration Pathways (RCPs) and their uncertainty. Climatic Change 128. https://doi.org/10.1007/s10584-014-1290-1.

Leung, L.R., Gustafson Jr., W.I., 2005. Potential regional climate change and implications to U.S. air quality. Geophys. Res. Lett. 32 https://doi.org/10.1029/2005gl022911.

Li, M., Liu, H., Geng, G., Hong, C., Liu, F., Song, Y., Tong, D., Zheng, B., Cui, H., Man, H., Zhang, Q., He, K., 2017. Anthropogenic emission inventories in China: a review. National Science Review 4, 834–866. https://doi.org/10.1093/nsr/nwx150.

Li, M., Wang, L., Liu, J., Gao, W., Song, T., Sun, Y., Li, L., Li, X., Wang, Y., Liu, L., Daellenbach, K.R., Paasonen, P.J., Kerminen, V.-M., Kulmala, M., Wang, Y., 2020. Exploring the regional pollution characteristics and meteorological formation mechanism of PM2.5 in North China during 2013-2017. Environ. Int. 134 https://doi.org/10.1016/j.envint.2019.105283.

Li, X., Hu, X., Shi, S., Shen, L., Luan, L., Ma, Y., 2019. Spatiotemporal variations and

regional transport of air pollutants in two urban agglomerations in Northeast China plain. Chin. Geogr. Sci. 29, 917–933. https://doi.org/10.1007/s11769-019-1081-8.

Liao, T., Gui, K., Jiang, W., Wang, S., Wang, B., Zeng, Z., Che, H., Wang, Y., Sun, Y., 2018. Air stagnation and its impact on air quality during winter in Sichuan and Chongqing, southwestern China. Sci. Total Environ. 635, 576–585. https://doi.org/10.1016/j.scitotenv.2018.04.122.

Liu, F., Zhang, Q., Ronald, J.v. d.A., Zheng, B., Tong, D., Yan, L., Zheng, Y., He, K., 2016. Recent reduction in NOx emissions over China: synthesis of satellite observations and emission inventories. Environ. Res. Lett. 11 https://doi.org/10.1088/1748-9326/11/11/114002.

Luo, Y., Mengfan, T., Kun, Y., Yu, Z., Xiaolu, Z., Miao, Z., Yan, S., 2019. Research on PM2.5 estimation and prediction method and changing characteristics analysis under long temporal and large spatial scale - a case study in China typical regions. Sci. Total Environ. 696, 133983. https://doi.org/10.1016/j.scitotenv.2019.133983.

Ma, M., Gao, Y., Wang, Y., Zhang, S., Leung, L., Liu, C., Wang, S., Zhao, B., Chang, X., Su, H., Zhang, T., Sheng, L., Yao, X., Gao, H., 2019. Substantial ozone enhancement over the North China Plain from increased biogenic emissions due to heat waves and land cover in summer 2017. Atmos. Chem. Phys. Discuss. 1–27 https://doi.org/10.5194/acp-2019-362.

MEEPRC, 2012. Technical regulation on ambient air quality index (on trial): HJ 633. Available at. http://www.mee.gov.cn/ywgz/fgbz/bz/bzwb/jcffbz/201203/W020120410332725219541.pdf. (Accessed 1 May 2020).

Mu, Q., Zhang, S.Q., 2013. An evaluation of the economic loss due to the heavy haze during January 2013 in China. China Environental Science 33, 2087–94.

Sun, J., Fu, J., Huang, K., Gao, Y., 2015. Estimation of future PM2.5- and ozone-related mortality over the continental United States in a changing climate: an application of high-resolution dynamical downscaling technique. J. Air Waste Manag. Assoc. 65, 611–623. https://doi.org/10.1080/10962247.2015.1033068.

Tan, J., Fu, J.S., Huang, K., Yang, C.-E., Zhuang, G., Sun, J., 2017. Effectiveness of SO2 emission control policy on power plants in the Yangtze River Delta, China-post-assessment of the 11th five-year plan. Environ. Sci. Pollut. Control Ser. 24, 8243–8255. https://doi.org/10.1007/s11356-017-8412-z.

Wang, J., Zhao, B., Wang, S., Yang, F., Xing, J., Morawska, L., Ding, A., Kulmala, M., Kerminen, V.-M., Kujansuu, J., Wang, Z., Ding, D., Zhang, X., Wang, H., Tian, M., Petaja, T., Jiang, J., Hao, J., 2017. Particulate matter pollution over China and the effects of control policies. Sci. Total Environ. 584, 426–447. https://doi.org/10.1016/j.scitotenv.2017.01.027.

Wang, J.X.L., Angell, J.K., 1999. Air Stagnation Climatology for the United States (1948-1998). NOAA/Air Resource Laboratory ATLAS, Silver Spring, USA.

Wang, S.X., Hao, J.M., 2012. Air quality management in China: issues, challenges, and options. J. Environ. Sci. China 24, 2–13. https://doi.org/10.1016/s1001-0742(11)60724-9.

Wang, X., Dickinson, R.E., Su, L., Zhou, C., Wang, K., 2018. PM2.5 pollution in China and how it has been exacerbated by terrain and meteorological conditions. Bull. Am. Meteorol. Soc. 99, 105–120. https://doi.org/10.1175/bams-d-16-0301.1.

Yin, Z., Wang, H., 2017. Role of atmospheric circulations in haze pollution in December 2016. Atmos. Chem. Phys. 17, 11673–11681. https://doi.org/10.5194/acp-17-11673-2017.

Yuan, T., Chen, S., Huang, J., Wu, D., Lu, H., Zhang, G., Ma, X., Chen, Z., Luo, Y., Ma, X., 2019. Influence of dynamic and thermal forcing on the meridional transport of Taklimakan Desert dust in spring and summer. J. Clim. 1 https://doi.org/10.1175/JCLI-D-18-0361.

Zeng, Y., Cao, Y., Qiao, X., Seyler, B.C., Tang, Y., 2019. Air pollution reduction in China: recent success but great challenge for the future. Sci. Total Environ. 663, 329–337. https://doi.org/10.1016/j.scitotenv.2019.01.262.

Zhang, G., Gao, Y., Cai, W., Leung, L.R., Wang, S., Zhao, B., Wang, M., Shan, H., Yao, X., Gao, H., 2019. Seesaw haze pollution in North China modulated by the sub-seasonal variability of atmospheric circulation. Atmos. Chem. Phys. 19, 565–576. https://doi.org/10.5194/acp-19-565-2019.

Zhang, J., Gao, Y., Luo, K., Leung, L., Zhang, Y., Wang, K., Fan, J., 2018. Impacts of compound extreme weather events on ozone in the present and future. Atmos. Chem. Phys. 18, 9861–9877. https://doi.org/10.5194/acp-18-9861-2018.

Zhao, B., Wang, S., Wang, J., Fu, J.S., Liu, T., Xu, J., Fu, X., Hao, J., 2013. Impact of national NOx and SO2 control policies on particulate matter pollution in China, Atmos. Environ. Times 77, 453–463. https://doi.org/10.1016/j.atmosenv.2013.05.012.

Zheng, B., Zhang, Q., Zhang, Y., He, K.B., Wang, K., Zheng, G.J., Duan, F.K., Ma, Y.L., Kimoto, T., 2015. Heterogeneous chemistry: a mechanism missing in current models to explain secondary inorganic aerosol formation during the January 2013 haze episode in North China. Atmos. Chem. Phys. 15, 2031–2049. https://doi.org/10.5194/acp-15-2031-2015.

Zhou, Y., Wu, Y., Yang, L., Fu, L., He, K., Wang, S., Hao, J., Chen, J., Li, C., 2010. The impact of transportation control measures on emission reductions during the 2008 Olympic Games in Beijing, China, Atmos. Environ. Times 44, 285–293. https://doi.org/10.1016/j.atmosenv.2009.10.040.